Preprints of the 21st IFAC World Congress (Virtual)
Berlin, Germany, July 12-17, 2020

Bearing-Only Formation Control of Multi-Agent System Without Leader's Velocity Information ⋆

Hongyu Ji[1] Quan Yuan[1,2] Cong Li[1,2,3] Xiang Li[1,2,3]

[1] *Adaptive Networks and Control Lab, Electronic Engineering Department, Fudan University, Shanghai, 200433, China*
[2] *Research Center of Smart Networks and Systems, School of Information Science and Engineering, Fudan University*
[3] *MOE Frontiers Center for Brain Science, Institute of Brain Science, Fudan University*

Abstract: This paper studies formation control of multi-agent systems with an underlying network constructed by defined the follower Henneberg construction. We propose a bearing-only formation control law of multi-agent systems, where a leader moves at a constant velocity, and the followers are unaware of the leader's velocity. We prove that the system can asymptotically reach its desired position and form the target formation. The proposed control law scales the formation to avoid obstacles, where the formation robustness is also analysed. Numerical simulations are provided to further support our findings.

Keywords: Formation control, bearing-only, multi-agent systems.

1. INTRODUCTION

Cooperative control of multi-agent systems has been studied widely due to its theoretical and practical significance. Formation control, as an important part of cooperative control of multi-agent systems, has shown broad application prospects, for example, formation navigation of autonomous vehicles (see Balch and Arkin (1998), Skjetne et al. (2002), Scharf et al. (2004) and Ren and Sorensen (2008)). Position-based, displacement-based and distance-based formation control have been widely studied (see Oh et al. (2015), Oh and Ahn (2011a), Oh and Ahn (2011b) and Dimarogonas and Johansson (2009)). Oh et al. (2015) concluded that position-based, displacement-based and distance-based control have a trade-off between the level of interactions among agents and the requirement in the sensing capability of individual agents. Compared to the above three solutions, bearing-only formation control attracts much attention due to the simplicity and low cost of the sensor system associated with the bearing measurements (see Van Tran et al. (2019)). It is a relatively new topic and has not been studied adequately yet.

The literatures of bearing-only formation control have paid attention to control the subtended bearing angle and the bearing rigidity (see Zhao et al. (2014), Basiri et al. (2010) and Jin (2016)). Basiri et al. (2010) studied the coupled bearing-only formation control of three mobile agents moving in the plane. Zhao et al. (2014) studied the distributed control of multi-vehicle formations with angle constraints using bearing-only measurements, whose target formation is cyclic, and the underlying information flow is undirected. To solve different formation control problems, Bishop et al. (2015) designed a distributed control scheme with bearing, distance and mixed bearing and distance constrains. In Zhao and Zelazo (2015), the theory of bearing rigidity and infinitesimal bearing rigidity was developed. Trinh et al. (2016) and Trinh et al. (2018) proposed a bearing-only control law with leader-first-follower formations, and analysed the stability of the formations as well as rotating and rescaling transformation of the target formation. In addition, Zhao and Zelazo (2019) studied bearing-only formation control with moving leaders and undirected underlying graph, which was not the leader-first-follower structure. Zhao and Zelazo (2019) systematically summarized the bearing rigidity theory and its applications for control and estimation of network systems. However, the formation control with a moving leader has not been fully studied. We here study the bearing-only formation control with leader-follower structure, where a leader moves at a constant velocity, and the followers are unaware of the leader's velocity.

We define a follower Henneberg construction to establish the interaction of multi-agent systems. Moreover, we study the bearing-only formation control laws and indicate the methods to rescale the target formation. In our system, the leader has a constant reference velocity. The followers assume a constant velocity of the leader, and adaptively estimate the reference velocity, which is not provided to them. Due to the target formation being fixed, controlling the leader's velocity to determine the position of the leader yields the control of the position to the target formation. Finally, we define a criterion R to test the robustness of the formation and explain the results.

⋆ This work was partly supported by National Natural Science Foundation of China (No. 61751303) and the National Natural Science Fund for Distinguished Young Scholar of China (No. 61425019).

The remainder of this paper is organized as follows. In section 2, we introduce an interaction network and analyse the controllability of the structure, which is generated by the follower Henneberg construction. In section 3, we prove the asymptotic formation stability of the multi-agent systems with a moving leader driven by our proposed bearing-only control laws. In section 4, we analyse the robustness of the formation. Numerical simulations to support the results are also provided. In section 5, we summarize this paper and outlook some future works.

2. PRELIMINARIES

Denote $G = (V, E)$ a directed graph with the vertex set $V = \{v_1, v_2, \ldots, v_n\}$ of n vertices and the edge set $E = \{e_{ij} = (v_i, v_j) | v_i, v_j \in V, v_i \neq v_j\}$ of m directed edges. e_{ij} is a directed edge pointing from i to j. Vertex j is a neighbour of vertex i if $e_{ij} \in E$. A directed path is a sequence of edges $(v_{i1}, v_{i2}), (v_{i2}, v_{i3}) \cdots (v_{i(k-1)}, v_{ik})$ in E. For expression clarity, we define $V_i = \{v_1, v_2, \cdots, v_i | v_j \in V, 1 \leq j \leq i, i \leq n\}$ the subset of the first i vertices e.g. $V_5 = \{v_1, v_2, v_3, v_4, v_5\}$.

Definition 1 (Follower Henneberg construction): For a graph with n vertices, starting from a directed edge e_{21} from vertex v_2 to v_1, each newly added vertex v_i $(i > 2)$ connects to vertex $v_{(i-1)}$ and vertex $v_{(i-2)}$, forming edges $e_{i(i-1)}$ and $e_{i(i-2)}$. A graph with n vertices and $(2n-3)$ edges is obtained. At each vertex addition, V_k spans at most $(2k-3)$ edges.

A graph with n vertices is a minimally rigid graph if and only if there are $(2n-3)$ edges in the graph (see Maxwell (1864), Laman (1970) and Henneberg (1911)). The minimally rigid graph has a Henneberg construction. The follower Henneberg construction, which is introduced in Definition 1, is a special Henneberg construction with cascade structure. Fig. 1 gives an example of the follower Henneberg construction on a graph with five vertices. Each vertex and its two neighbours form a triangle. If the triangle could be controlled to a desired position, the control laws can be generalized to any graph (Shen et al. (2014) and Guo et al. (2010)). The target formation is easy to implement with the cascade structure, where if agent i has reached its desired position, agent 1, agent 2,..., and agent $(i-1)$ must have also reached their desired positions.

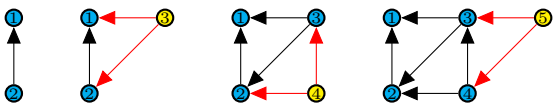

Fig. 1. An example of follower Henneberg construction with five vertices and seven edges. Red edges and yellow vertices are newly added at each step. The neighbour of vertex 2 is vertex 1. The neighbours of vertex i $(i > 2)$ are vertex $(i-1)$ and vertex $(i-2)$. This is a rigid graph because the number of vertices and edges satisfies $2 \times 5 - 3 = 7$.

We generate the interaction network of our multi-agent system with follower Henneberg construction. A vertex and a directed edge in the interaction network respectively represent an agent and the information flow between two agents in the multi-agent system. A directed edge e_{ij} from v_j to v_i means agent j can obtain the position information of agent i.

In a 3D Euclidean space, we associate the position of each vertex v_i at time t with a point $\mathbf{p}_i(t)$. The stacked vector $\mathbf{p}(t) = [\mathbf{p}_1(t)^\intercal, \mathbf{p}_2(t)^\intercal, \cdots, \mathbf{p}_n(t)^\intercal]^\intercal \in \mathbb{R}^{3n}$ is referred to as a configuration of G (see Trinh et al. (2018)). Similarly, the desired position of vertex $\mathbf{v}_i$ is also associated with a desired point $\mathbf{p}_i^*(t) \in \mathbb{R}^3$. $\mathbf{p}^*(t) = [\mathbf{p}_1^*(t)^\intercal, \mathbf{p}_2^*(t)^\intercal, \cdots, \mathbf{p}_n^*(t)^\intercal]^\intercal \in \mathbb{R}^{3n}$. The formation control target is to drive all the agents to a pre-set target formation and positions, satisfying $\lim_{t\to\infty} \|\mathbf{p}_i(t) - \mathbf{p}_i^*(t)\| = 0$, $\lim_{t\to\infty} \|\dot{\mathbf{p}}_i(t) - \dot{\mathbf{p}}_i{}^*(t)\| = 0$ for all n agents in the system.

At time t, $\mathbf{z}_{ij}(t) := \mathbf{p}_j(t) - \mathbf{p}_i(t)$ is the direction vector between agent i and agent j. The bearing vector is obtained by normalizing $\mathbf{z}_{ij}(t)$:

$$\mathbf{g}_{ij}(t) = \frac{\mathbf{p}_j(t) - \mathbf{p}_i(t)}{\|\mathbf{p}_j(t) - \mathbf{p}_i(t)\|} = \frac{\mathbf{z}_{ij}(t)}{\|\mathbf{z}_{ij}(t)\|} \in \mathbb{R}^3 \tag{1}$$

Let $\Gamma := \{\mathbf{g}_{21}^*, \mathbf{g}_{31}^*, \cdots, \mathbf{g}_{ij}^* | (v_i, v_j) \in E\}$ be the set of pre-set bearing vectors in the target formation. Bearing vectors of the multi-agent system's interaction network are the same as those in set Γ. Note that all agents share the same reference frame.

3. CONTROL LAW DESIGN

Consider a multi-agent system with n agents in 3D Euclidean space, each agent is modelled with single-integrator dynamics:

$$\dot{\mathbf{p}}_i(t) = \mathbf{u}_i(t) \tag{2}$$

where $\mathbf{p}_i(t) \in \mathbb{R}^3$ is the position of agent i and $\mathbf{u}_i(t) \in \mathbb{R}^3$ is the control input of agent i.

To formulate the formation control problem, we establish the following three assumptions:

Assumption 1: The target formation is pre-set with a set of desired bearings $\Gamma := \{\mathbf{g}_{21}^*, \mathbf{g}_{31}^*, \cdots, \mathbf{g}_{ij}^* | (v_i, v_j) \in E\}$, and the desired distance between the leader (agent 1) and the first follower (agent 2) is d_{21}^*.

Assumption 2: An agent $i\,(2 < i \leq n)$ can measure the unit direction vectors $\mathbf{g}_{i(i-1)}$ and $\mathbf{g}_{i(i-2)}$ between itself and its two neighbours. Moreover, the first follower knows the desired distance d_{21}^* between itself and the leader in the target formation.

Assumption 3: The leader has a constant reference velocity $\mathbf{v}_0 \in \mathbb{R}^3$. The followers are unaware of the reference velocity directly, but they can estimate it from known bearing information.

The formation control problem is formulated as follows:

1) For $i = 1$, $\lim_{t\to\infty} \|\dot{\mathbf{p}}_1(t) - \mathbf{v}_0\| = 0$.
2) For $i = 2$, $\lim_{t\to\infty} \|\dot{\mathbf{p}}_2(t) - \mathbf{v}_0\| = 0$, $\lim_{t\to\infty} \|\mathbf{g}_{12}(t) - \mathbf{g}_{12}^*\| = 0$.
3) For $i > 2$, $\lim_{t\to\infty} \|\dot{\mathbf{p}}_i(t) - \mathbf{v}_0\| = 0$, $\lim_{t\to\infty} \|\mathbf{g}_{i(i-1)}(t) - \mathbf{g}_{i(i-1)}^*\| = 0$, $\lim_{t\to\infty} \|\mathbf{g}_{i(i-2)}(t) - \mathbf{g}_{i(i-2)}^*\| = 0$

Definition 2: Let $\mathbf{e} = [e_1, e_2, e_3] \in \mathbb{R}^3$ be a vector in 3D Euclidean space. The orthogonal projection matrix of a

non-zero vector $\mathbf{e}$ is defined as (see Trinh et al. (2016) and Trinh et al. (2018))

$$\mathbf{P}_e = \mathbf{I} - \frac{\mathbf{e}}{\|\mathbf{e}\|}\frac{\mathbf{e}^\intercal}{\|\mathbf{e}^\intercal\|} \in \mathbb{R}^{3\times 3} \tag{3}$$

The leader is the driver vertex in the interaction network, and the position of the target formation depends on the leader's reference velocity $\mathbf{v}_0$ and the leader's initial position $\mathbf{p}_1(0)$. The control law for the leader is:

$$\dot{\mathbf{p}_1}(t) = \mathbf{v}_0 \tag{4}$$

The velocity of the leader is constant but the desired position is time-variant. Assume that the desired position of the leader in initial state is $\mathbf{p}_1^*(0)$. At time t, the desired position of the leader is

$$\mathbf{p}_1^*(t) = \mathbf{p}_1^*(0) + \mathbf{v}_0 t \tag{5}$$

The first follower's desired position is

$$\mathbf{p}_2^*(t) = \mathbf{p}_1^*(t) - \mathbf{g}_{21}^* d_{21}^* \tag{6}$$

Other followers' desired position is calculated in Trinh et al. (2018):

$$\begin{aligned}\mathbf{p}_i^*(t) =&(\mathbf{P}_{\mathbf{g}_{ij}^*} + \mathbf{P}_{\mathbf{g}_{ik}^*})^{-1}(\mathbf{P}_{\mathbf{g}_{ij}^*}\mathbf{p}_j^*(t) + \mathbf{P}_{\mathbf{g}_{ik}^*}\mathbf{p}_k^*(t)) \\ &(j = i-1, k = i-2)\end{aligned} \tag{7}$$

The first follower has the leader as its only neighbour. The control law for the first follower is :

$$\dot{\mathbf{p}_2}(t) = -\mathbf{P}_{\mathbf{g}_{21}(t)}\big(\alpha\mathbf{g}_{21}^* + \int_0^t \beta(\tau)(\mathbf{g}_{21}(\tau) - \mathbf{g}_{21}^*)d\tau\big) \tag{8}$$

The item $\int_0^t \beta(\tau)(\mathbf{g}_{21}(\tau) - \mathbf{g}_{21}^*)d\tau$ is the time-variant error between the current position and the desired position of the first follower, and $\beta(t)$ is the speed of agent 2 at time t. At time $t(t>0)$, $\mathbf{p}_2(t)$ always converges to $\mathbf{p}_2^*(t)$. Consider the Lyapunov function $V_2 = \frac{1}{2}\| \mathbf{p}_2(t) - \mathbf{p}_2^*(t) \|^2$, where V_2 is positive definite and $V_2 = 0$ if and only if $\mathbf{p}_2(t) = \mathbf{p}_2^*(t)$. Besides, the derivative of V_2 is

$$\begin{aligned}\dot{V_2} &= (\mathbf{p}_2(t) - \mathbf{p}_2^*(t))^\intercal \dot{\mathbf{p}}_2(t) \\ &= -\alpha(\mathbf{p}_2(t) - \mathbf{p}_2^*(t))^\intercal \mathbf{P}_{\mathbf{g}_{21}(t)}\mathbf{g}_{21}^* \\ &\quad - (\mathbf{p}_2(t) - \mathbf{p}_2^*(t))^\intercal \mathbf{P}_{\mathbf{g}_{21}(t)} \int_0^t \beta(\tau)(\mathbf{g}_{21}(\tau) - \mathbf{g}_{21}^*)d\tau \\ &= -\alpha(\mathbf{p}_2(t) - \mathbf{p}_2^*(t))^\intercal \frac{\mathbf{P}_{\mathbf{g}_{21}(t)}}{d_{21}^*}(\mathbf{p}_2(t) - \mathbf{p}_2^*(t)) \\ &\quad - (\mathbf{p}_2(t) - \mathbf{p}_2^*(t))^\intercal \mathbf{P}_{\mathbf{g}_{21}(t)}(\mathbf{p}_2(t) - \mathbf{p}_2^*(t)) \\ &\quad - (\mathbf{p}_2(t) - \mathbf{p}_2^*(t))^\intercal \mathbf{P}_{\mathbf{g}_{21}(t)}(\mathbf{p}_2^*(0) - \mathbf{p}_2(0)) \\ &= -(\frac{\alpha}{d_{21}^*} + 1)(\mathbf{p}_2(t) - \mathbf{p}_2^*(t))^\intercal \mathbf{P}_{\mathbf{g}_{21}(t)}(\mathbf{p}_2(t) - \mathbf{p}_2^*(t)) \\ &\quad + (\mathbf{p}_2(t) - \mathbf{p}_2^*(t))^\intercal \mathbf{P}_{\mathbf{g}_{21}(t)}(\mathbf{p}_2(0) - \mathbf{p}_2^*(0)) \\ &\leqslant -(\frac{\alpha}{d_{21}^*} + 1)(\mathbf{p}_2(t) - \mathbf{p}_2^*(t))^\intercal \mathbf{P}_{\mathbf{g}_{21}(t)}(\mathbf{p}_2(t) - \mathbf{p}_2^*(t)) \\ &\quad + \| \mathbf{p}_2(t) - \mathbf{p}_2^*(t) \| \| \mathbf{P}_{\mathbf{g}_{21}(t)} \| \| \mathbf{p}_2(0) - \mathbf{p}_2^*(0) \| \\ &\leqslant -(\frac{\alpha}{d_{21}^*} + 1)(\mathbf{p}_2(t) - \mathbf{p}_2^*(t))^\intercal \mathbf{P}_{\mathbf{g}_{21}(t)}(\mathbf{p}_2(t) - \mathbf{p}_2^*(t)) \\ &\quad + \| \mathbf{p}_2(t) - \mathbf{p}_2^*(t) \| \| \mathbf{P}_{\mathbf{g}_{21}(t)} \| (d_{21} + d_{21}^*)\end{aligned} \tag{9}$$

$\dot{V_2} = 0$ if and only if $\mathbf{p}_2(t) - \mathbf{p}_2^*(t) = 0$. When $\alpha > 0$ and $\mathbf{p}_2(t)$ is large, the second term can be ignored. Therefore, when $\alpha > 0$, $\dot{V_2} < 0$, $\mathbf{p}_2(t)$ converges to $\mathbf{p}_2^*(t)$.

The second follower has two neighbours, which are the leader and the first follower. The control law for the second follower is:

$$\begin{aligned}\dot{\mathbf{p}_3}(t) = &-\mathbf{P}_{\mathbf{g}_{31}(t)}\big(\alpha\mathbf{g}_{31}^* + \int_0^t \beta(\tau)(\mathbf{g}_{31}(\tau) - \mathbf{g}_{31}^*)d\tau\big) \\ &- \mathbf{P}_{\mathbf{g}_{32}(t)}\big(\alpha\mathbf{g}_{32}^* + \int_0^t \beta(\tau)(\mathbf{g}_{32}(\tau) - \mathbf{g}_{32}^*)d\tau\big)\end{aligned} \tag{10}$$

The position of the second follower is determined by the leader's position and the first follower's position together. Its initial position has no limitations. At time $t(t>0)$, $\mathbf{p}_3(t)$ always converges to $\mathbf{p}_3^*(t)$. Consider the Lyapunov function $V_3 = \frac{1}{2}\| \mathbf{p}_3(t) - \mathbf{p}_3^*(t) \|^2$, where V_3 is positive definite and $V_3 = 0$ if and only if $\mathbf{p}_3(t) = \mathbf{p}_3^*(t)$. Moreover, the derivative of V_3 is

$$\begin{aligned}\dot{V_3} &= (\mathbf{p}_3(t) - \mathbf{p}_3^*(t))^\intercal \dot{\mathbf{p}}_3(t) \\ &= -\alpha(\mathbf{p}_3(t) - \mathbf{p}_3^*(t))^\intercal(\mathbf{P}_{\mathbf{g}_{32}(t)}\mathbf{g}_{32}^* + \mathbf{P}_{\mathbf{g}_{31}(t)}\mathbf{g}_{31}^*) \\ &\quad - (\mathbf{p}_3(t) - \mathbf{p}_3^*(t))^\intercal \mathbf{P}_{\mathbf{g}_{32}(t)} \int_0^t \beta(\tau)(\mathbf{g}_{32}(\tau) - \mathbf{g}_{32}^*)d\tau \\ &\quad - (\mathbf{p}_3(t) - \mathbf{p}_3^*(t))^\intercal \mathbf{P}_{\mathbf{g}_{31}(t)} \int_0^t \beta(\tau)(\mathbf{g}_{31}(\tau) - \mathbf{g}_{31}^*)d\tau) \\ &= -\alpha(\mathbf{p}_3(t) - \mathbf{p}_3^*(t))^\intercal(\frac{\mathbf{P}_{\mathbf{g}_{32}(t)}}{\| z_{32}^* \|} + \frac{\mathbf{P}_{\mathbf{g}_{31}(t)}}{\| z_{31}^* \|})(\mathbf{p}_3(t) - \mathbf{p}_3^*(t)) \\ &\quad - (\mathbf{p}_3(t) - \mathbf{p}_3^*(t))^\intercal \mathbf{P}_{\mathbf{g}_{32}(t)}(\mathbf{p}_3(t) - \mathbf{p}_3^*(t)) \\ &\quad - (\mathbf{p}_3(t) - \mathbf{p}_3^*(t))^\intercal \mathbf{P}_{\mathbf{g}_{32}(t)}(\mathbf{p}_3^*(0) - \mathbf{p}_3(0)) \\ &\quad - (\mathbf{p}_3(t) - \mathbf{p}_3^*(t))^\intercal \mathbf{P}_{\mathbf{g}_{31}(t)}(\mathbf{p}_3(t) - \mathbf{p}_3^*(t)) \\ &\quad - (\mathbf{p}_3(t) - \mathbf{p}_3^*(t))^\intercal \mathbf{P}_{\mathbf{g}_{31}(t)}(\mathbf{p}_3^*(0) - \mathbf{p}_3(0)) \\ &= -(\mathbf{p}_3(t) - \mathbf{p}_3^*(t))^\intercal \mathbf{P}_{\mathbf{g}_{32}(t)}(\frac{\alpha}{\| z_{32}^* \|} + 1)(\mathbf{p}_3(t) - \mathbf{p}_3^*(t)) \\ &\quad - (\mathbf{p}_3(t) - \mathbf{p}_3^*(t))^\intercal \mathbf{P}_{\mathbf{g}_{31}(t)}(\frac{\alpha}{\| z_{31}^* \|} + 1)(\mathbf{p}_3(t) - \mathbf{p}_3^*(t)) \\ &\quad + (\mathbf{p}_3(t) - \mathbf{p}_3^*(t))^\intercal(\mathbf{P}_{\mathbf{g}_{32}(t)} + \mathbf{P}_{\mathbf{g}_{31}(t)})(\mathbf{p}_3(0) - \mathbf{p}_3^*(0)) \\ &\leqslant -(\mathbf{p}_3(t) - \mathbf{p}_3^*(t))^\intercal \mathbf{P}_{\mathbf{g}_{32}(t)}(\frac{\alpha}{\| z_{32}^* \|} + 1)(\mathbf{p}_3(t) - \mathbf{p}_3^*(t)) \\ &\quad - (\mathbf{p}_3(t) - \mathbf{p}_3^*(t))^\intercal \mathbf{P}_{\mathbf{g}_{31}(t)}(\frac{\alpha}{\| z_{31}^* \|} + 1)(\mathbf{p}_3(t) - \mathbf{p}_3^*(t)) \\ &\quad + \| \mathbf{p}_3(t) - \mathbf{p}_3^*(t) \| \| \mathbf{P}_{\mathbf{g}_{32}(t)} + \mathbf{P}_{\mathbf{g}_{31}(t)} \| max\{z_{32} + \\ &\quad z_{32}^*, z_{31} + z_{31}^*\}\end{aligned} \tag{11}$$

$\dot{V_3} = 0$ if and only if $\mathbf{p}_3(t) - \mathbf{p}_3^*(t) = 0$. When $\alpha > 0$ and $\mathbf{p}_3(t)$ is large, the third term can be ignored. Therefore, when $\alpha > 0$, $\dot{V_3} < 0$, $\mathbf{p}_3(t)$ converges to $\mathbf{p}_3^*(t)$.

Similarly, for the other followers, the neighbours of agent i are agent $(i-1)$ and agent $(i-2)$ $(i = 3, 4, 5, \ldots, n)$. Note $j = i-1, k = i-2$. The control law for agent i is

$$\begin{aligned}\dot{\mathbf{p}_i}(t) = &-\mathbf{P}_{\mathbf{g}_{ij}(t)}\big(\alpha\mathbf{g}_{ij}^* + \int_0^t \beta(\tau)(\mathbf{g}_{ij}(\tau) - \mathbf{g}_{ij}^*)d\tau\big) \\ &- \mathbf{P}_{\mathbf{g}_{ik}(t)}\big(\alpha\mathbf{g}_{ik}^* + \int_0^t \beta(\tau)(\mathbf{g}_{ik}(\tau) - \mathbf{g}_{ik}^*)d\tau\big)\end{aligned} \tag{12}$$

Considering an n-agent system, the dynamics of each agent can be expressed as

$$\dot{\mathbf{p}}(t) = \begin{bmatrix} \dot{\mathbf{p}}_1(t) \\ \dot{\mathbf{p}}_2(t) \\ \vdots \\ \dot{\mathbf{p}}_i(t) \\ \vdots \\ \dot{\mathbf{p}}_n(t) \end{bmatrix} \tag{13}$$

where $\dot{\mathbf{p}}_i(t)$ is the input control of agent i as shown in (4), (8), (10) and (12). We give the following theorem.

Theorem 1: For a multi-agent system (13) whose interaction network is constructed by follower Henneberg construction, under Assumptions 1-3 and the proposed control laws (4), (8), (10) and (12), the agents in the system will asymptotically reach their desired positions $\mathbf{p}^*(t) = [\mathbf{p}_1^*(t)^\intercal, \mathbf{p}_2^*(t)^\intercal, \cdots, \mathbf{p}_n^*(t)^\intercal]^\intercal$.

Proof: We use mathematical induction to prove this theorem. Firstly, for $i = 1$, at any time, the leader's present position is its desired position.

Secondly, for $i = 2$ and $i = 3$, as shown as (9) and (11), Theorem 1 is true.

Thirdly, for $4 \leqslant i \leqslant n$, consider the Lyapunov function $V_i = \frac{1}{2} \| \mathbf{p}_i(t) - \mathbf{p}_i^*(t) \|^2$, where V_i is positive definite and $V_i = 0$ if and only $\mathbf{p}_i(t) = \mathbf{p}_i^*(t)$. The derivative of V_i is

$$
\begin{aligned}
\dot{V}_i &= (\mathbf{p}_i(t) - \mathbf{p}_i^*(t))^\intercal \dot{\mathbf{p}}_i(t) \\
&= -\alpha(\mathbf{p}_i(t) - \mathbf{p}_i^*(t))^\intercal (\mathbf{P}_{\mathbf{g}_{ij}(t)} \mathbf{g}_{ij}^* + \mathbf{P}_{\mathbf{g}_{ik}(t)} \mathbf{g}_{ik}^*) \\
&\quad - (\mathbf{p}_i(t) - \mathbf{p}_i^*(t))^\intercal \mathbf{P}_{\mathbf{g}_{ij}(t)} \int_0^t \beta(\tau)(\mathbf{g}_{ij}(\tau) - \mathbf{g}_{ij}^*) d\tau \\
&\quad - (\mathbf{p}_i(t) - \mathbf{p}_i^*(t))^\intercal \mathbf{P}_{\mathbf{g}_{ik}(t)} \int_0^t \beta(\tau)(\mathbf{g}_{ik}(\tau) - \mathbf{g}_{ik}^*) d\tau) \\
&= -\alpha(\mathbf{p}_i(t) - \mathbf{p}_i^*(t))^\intercal (\frac{\mathbf{P}_{\mathbf{g}_{ij}(t)}}{\| z_{ij}^* \|} + \frac{\mathbf{P}_{\mathbf{g}_{ik}(t)}}{\| z_{ik}^* \|})(\mathbf{p}_i(t) - \mathbf{p}_i^*(t)) \\
&\quad - (\mathbf{p}_i(t) - \mathbf{p}_i^*(t))^\intercal \mathbf{P}_{\mathbf{g}_{ij}(t)} (\mathbf{p}_i(t) - \mathbf{p}_i^*(t)) \\
&\quad - (\mathbf{p}_i(t) - \mathbf{p}_i^*(t))^\intercal \mathbf{P}_{\mathbf{g}_{ij}(t)} (\mathbf{p}_i^*(0) - \mathbf{p}_i(0)) \\
&\quad - (\mathbf{p}_i(t) - \mathbf{p}_i^*(t))^\intercal \mathbf{P}_{\mathbf{g}_{ik}(t)} (\mathbf{p}_i(t) - \mathbf{p}_i^*(t)) \\
&\quad - (\mathbf{p}_i(t) - \mathbf{p}_i^*(t))^\intercal \mathbf{P}_{\mathbf{g}_{ik}(t)} (\mathbf{p}_i^*(0) - \mathbf{p}_i(0)) \\
&= -(\mathbf{p}_i(t) - \mathbf{p}_i^*(t))^\intercal \mathbf{P}_{\mathbf{g}_{ij}(t)} (\frac{\alpha}{\| z_{ij}^* \|} + 1)(\mathbf{p}_i(t) - \mathbf{p}_i^*(t)) \\
&\quad - (\mathbf{p}_i(t) - \mathbf{p}_i^*(t))^\intercal \mathbf{P}_{\mathbf{g}_{ik}(t)} (\frac{\alpha}{\| z_{ik}^* \|} + 1)(\mathbf{p}_i(t) - \mathbf{p}_i^*(t)) \\
&\quad + (\mathbf{p}_i(t) - \mathbf{p}_i^*(t))^\intercal (\mathbf{P}_{\mathbf{g}_{ij}(t)} + \mathbf{P}_{\mathbf{g}_{ik}(t)})(\mathbf{p}_i(t) - \mathbf{p}_i^*(t)) \\
&\leqslant -(\mathbf{p}_i(t) - \mathbf{p}_i^*(t))^\intercal \mathbf{P}_{\mathbf{g}_{ij}(t)} (\frac{\alpha}{\| z_{ij}^* \|} + 1)(\mathbf{p}_i(t) - \mathbf{p}_i^*(t)) \\
&\quad - (\mathbf{p}_i(t) - \mathbf{p}_i^*(t))^\intercal \mathbf{P}_{\mathbf{g}_{ik}(t)} (\frac{\alpha}{\| z_{ik}^* \|} + 1)(\mathbf{p}_i(t) - \mathbf{p}_i^*(t)) \\
&\quad + \| \mathbf{p}_i(t) - \mathbf{p}_i^*(t) \| \| \mathbf{P}_{\mathbf{g}_{ij}(t)} + \mathbf{P}_{\mathbf{g}_{ik}(t)} \| \, max\{z_{ij} + \\
&\quad z_{ij}^*, z_{ik} + z_{ik}^*\} \qquad (14)
\end{aligned}
$$

$\dot{V}_i = 0$ if and only if $\mathbf{p}_i(t) - \mathbf{p}_i^*(t) = 0$. When $\alpha > 0$ and $\mathbf{p}_i(t)$ is large, the third term can be ignored. Therefore, when $\alpha > 0$, $\dot{V}_i < 0$, $\mathbf{p}_i(t)$ converges to $\mathbf{p}_i^*(t)$.

Finally, through mathematical induction, the convergence also holds for $4 \leqslant i \leqslant n$. ■

In our system, the position of each follower is determined by its two neighbours, i.e. the position of agent i is determined by agents $(i-1)$ and $(i-2)$, and the position of agent $(i-1)$ is determined by agents $(i-2)$ and $(i-3)$, ..., the position of agent 2 is determined by agent 1. The position of agent 1 is directly determined by the reference velocity $\mathbf{v}_0$ and its initial position. In a nutshell, in this cascade structure, the desired position of agent i is indirectly determined by the reference velocity $\mathbf{v}_0$ and the leader's initial position.

The parameter α is designed based on the specific system environment, including the velocity of the leader, the scale of the target formation, the control precision, etc. Furthermore, α directly determines the scale of the target formation, which provides great convenience to rescale the target formation through input control. If the scale of the target formation is changed, agents' desired positions are also changed. It is beneficial to avoid the obstacles by controlling the scale of the to change agents' positions. If the moving agents detect obstacles ahead, it is feasible for the system to adjust the parameter α of input control to scale the formation to avoid obstacles.

4. NUMERICAL SIMULATIONS ON FORMATION ROBUSTNESS

Consider a multi-agent system with eight agents. Simulation results illustrate the effect of parameters α on rescaling of the final formation. The error between the agents' final positions and their desired positions are calculated from numerical simulations data. The error curve is fitted through linear and B-spline interpolation and the robustness of the formation is also discussed.

In Figs. 2, 3 and 4, curves of different colors show the trajectories of each agent with different choices of α. In the initial state, $\mathbf{p}_0 = [0, 0, 0]$ and $d_{21}^* = 4$. The desired bearings are $\mathbf{g}^* = \{[0, 1, 0], [1, 0, 0], [\frac{\sqrt{2}}{2}, -\frac{\sqrt{2}}{2}, 0], \ldots, [1, 0, 0], [0, 1, 0]\}$, which form a cube with an edge length of 4 given by d_{21}^*. The green dots are the initial positions of the agents randomly distributed within ([0,10],[0,10],[0,10]). The leader moves at a constant velocity of [0.2,0.2,0.2]. The yellow cube is the target formation when the leader is at its initial state and the desired terminal formation is shown with the magenta one. In the final formation, all desired bearing vectors are satisfied with different formation scales. The simulation results are consistent with the control laws (4), (8), (10) and (12) .

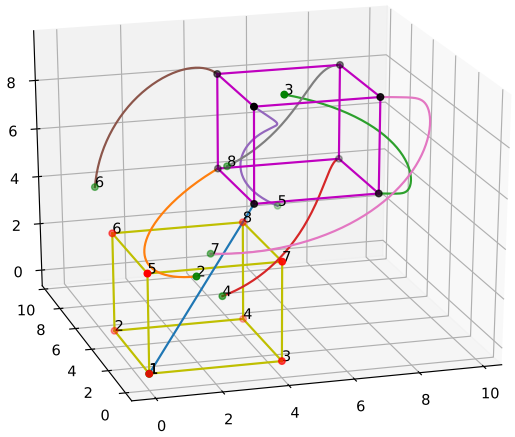

Fig. 2. The final target formation is the same as the initial target formation.

Parameter α determines the scale of the terminal formation. Fig.3 shows that the final formation (magenta

cube) is enlarged compared with the yellow cube (which is the pre-set target formation). However, in Fig.4, the final formation is shrunk.

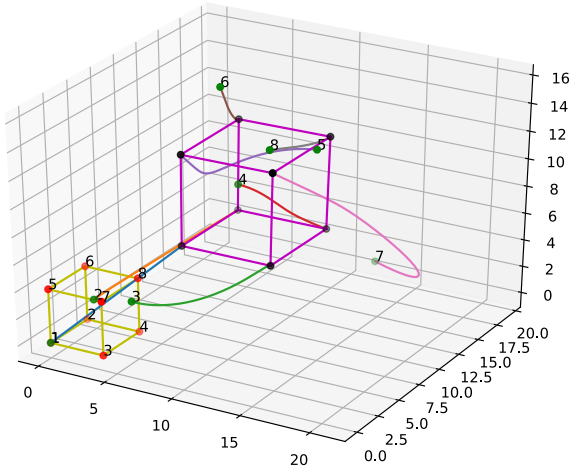

Fig. 3. The final target formation is larger than the initial target formation. The side length of the yellow cube is 4, however, it is 6 in the magenta cube.

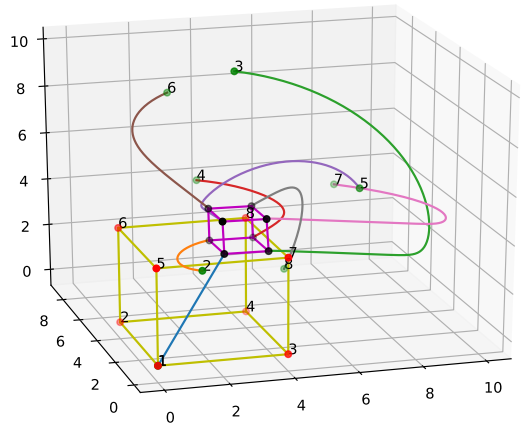

Fig. 4. The final target formation is smaller than the initial target formation. The side length of the yellow cube is 4, however, it is 1 in the magenta cube.

The formation accuracy with the mean-square error(MSE) between the final position $\mathbf{p}_i$ and the desired position $\mathbf{p}_i^*$ of each agent is

$$MSE(\mathbf{p}_i) = \frac{1}{3}\sum_{k=0}^{3}(p_i^{(k)} - p_i^{*(k)})^2 \tag{15}$$

In Fig. 5, x-axis is the index i of each agent and the y-axis is the error $MSE(\mathbf{p}_i)$. Fig. 5 shows that the error accumulates as the agent index goes higher.

Robustness is an essential criterion to evaluate relative stability of control law design. Dekker and Colbert (2004) defined the robustness as the ability of a network to continue to perform its functions in the face of attack, either random or targeted. Zeng and Liu (2012) mainly

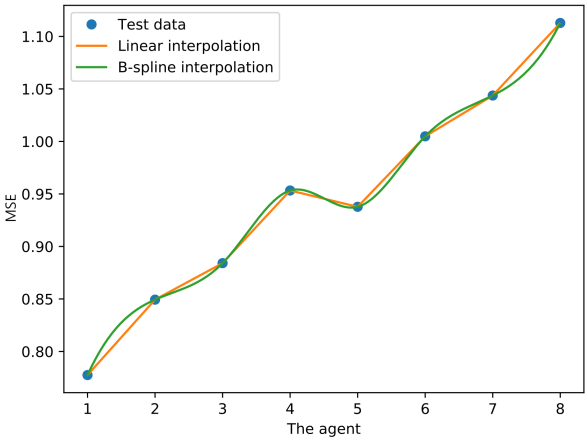

Fig. 5. Error Curve. The blue dots are test data of Fig. 2.

studied and optimized the robustness of nodes and edges. A hybrid defence model was specially designed to balance the relationship between the robustness of nodes and edges in Zeng and Liu (2012). In view of bearing-only formation control, we define a robustness criterion to evaluate the performance. During the formation control process, if $\mathbf{v}_0$ changes within a time duration Δt and we experiment m times, for agent i, it reaches its desired position m^* times, thus $\lambda_i = \frac{m^*}{m}$ and $\bar{\lambda} = \frac{1}{n}\sum_{i=1}^{n}\lambda_i$. For agent i, t_{ir} is the time needed to reach its desired position from being attacked and $\bar{t}_r = \frac{1}{n}\sum_{i=1}^{n} t_{ir}$. For the system (13), the criterion is defined by

$$R = \frac{\bar{\lambda}}{\bar{t}_r} \tag{16}$$

The criterion R increases with the increase of $\bar{\lambda}$ and decreases with the increase of $\bar{t}_r$. If $\bar{\lambda}$ is approximate to 1 but $\bar{t}_r$ is too large, the control performance may not be acceptable. The expected performance is that even when an instantaneous jitter happens to the reference velocity $\mathbf{v}_0$ within Δt, agents other than the leader should maintain the target formation or restore to the target formation within a reasonable period of time.

Table 1. Robustness test results

The robustness test data of Fig. 4.

	$\Delta t_1 = 1$		$\Delta t_2 = 2$		$\Delta t_3 = 5$		$\Delta t_4 = 10$	
	λ_i	t_{ir}	λ_i	t_{ir}	λ_i	t_{ir}	λ_i	t_{ir}
agent 1	1.00	5.27	1.00	4.27	1.00	1.27	1.00	1.24
agent 2	0.47	5.09	0.47	4.09	0.47	1.09	0.00	> 30
agent 3	0.48	8.93	0.72	0.28	0.68	0.46	0.00	> 30
agent 4	0.70	0.11	0.62	0.02	0.36	1.27	0.00	> 30
agent 5	0.63	5.86	0.46	6.12	0.54	29.03	0.00	> 30
agent 6	0.64	0.38	0.37	6.26	0.68	0.42	0.00	> 30
agent 7	0.30	1.34	0.28	0.04	0.24	39.8	0.00	> 30
agent 8	0.17	0.15	0	> 30	0.19	0.40	0.00	> 30
R	$R_1 = 0.16$		$R_2 \to 0$		$R_3 = 0.08$		$R_4 \to 0$	

Table 1 is the robustness test data under four cases. Test duration is 30 seconds. If an agent does not reach its desired position within 30 seconds, t_{ir} must be greater than 30s. If $t_{ir} > 30$, we cannot test the accurate time so

that we use $R \to 0$ to estimate poor performances. The robustness criterion R is calculated independently under different cases.

As shown in Table 1, when Δt is small, it is too short to adjust the change of the reference velocity for the multi-agent system. However, as shown in the forth test, when $\Delta t = 10s$, only the leader can reach its desired position within 30s. The followers cannot reach their desired positions within $30s$. It can be interpreted as that if Δt is larger than a threshold, the system adapts to move at the new velocity. Once the system gets back to the initial reference velocity, to the system, this change is a new attack.

5. CONCLUSION

We have investigated the bearing-only formation control of multi-agent systems with a moving leader. The interaction network is constructed by follower Henneberg construction. The control laws drive the system to reach the target formation as well as rescale it. We have proved that the multi-agent system asymptotically converges to its desired positions and target formation. Although we expound our research and results in 3D Euclidean space, it is also applicable to higher order spaces as long as the interaction network is rigid.

However, how to determine the parameters to control the scale of the final formation is not fully studied in this work. Future research includes the study of adaptive control laws of bearing-only formation control, which could adaptively control the scale of the target formation to avoid obstacle according to environment.

REFERENCES

Balch, T. and Arkin, R.C. (1998). Behavior-based formation control for multirobot teams. *IEEE transactions on robotics and automation*, 14(6), 926–939.

Basiri, M., Bishop, A.N., and Jensfelt, P. (2010). Distributed control of triangular formations with angle-only constraints. *Systems & Control Letters*, 59(2), 147–154.

Bishop, A.N., Deghat, M., Anderson, B.D., and Hong, Y. (2015). Distributed formation control with relaxed motion requirements. *International Journal of Robust and Nonlinear Control*, 25(17), 3210–3230.

Dekker, A.H. and Colbert, B.D. (2004). Network robustness and graph topology. In *Proceedings of the 27th Australasian conference on Computer science-Volume 26*, 359–368. Australian Computer Society, Inc.

Dimarogonas, D.V. and Johansson, K.H. (2009). Further results on the stability of distance-based multi-robot formations. In *2009 American Control Conference*, 2972–2977.

Guo, J., Lin, Z., Cao, M., and Yan, G. (2010). Adaptive leader-follower formation control for autonomous mobile robots. In *Proceedings of the 2010 American control conference*, 6822–6827.

Henneberg, L. (1911). *Die graphische Statik der starren Systeme*, volume 31. BG Teubner.

Jin, X. (2016). Fault tolerant finite-time leader–follower formation control for autonomous surface vessels with los range and angle constraints. *Automatica*, 68, 228–236.

Laman, G. (1970). On graphs and rigidity of plane skeletal structures. *Journal of Engineering mathematics*, 4(4), 331–340.

Maxwell, J.C. (1864). L. on the calculation of the equilibrium and stiffness of frames. *The London, Edinburgh, and Dublin Philosophical Magazine and Journal of Science*, 27(182), 294–299.

Oh, K.K. and Ahn, H.S. (2011a). Distance-based control of cycle-free persistent formations. In *2011 IEEE International Symposium on Intelligent Control*, 816–821.

Oh, K.K. and Ahn, H.S. (2011b). Distance-based formation control using euclidean distance dynamics matrix: Three-agent case. In *Proceedings of the 2011 American control conference*, 4810–4815.

Oh, K.K., Park, M.C., and Ahn, H.S. (2015). A survey of multi-agent formation control. *Automatica*, 53, 424–440.

Ren, W. and Sorensen, N. (2008). Distributed coordination architecture for multi-robot formation control. *Robotics and Autonomous Systems*, 56(4), 324–333.

Scharf, D.P., Hadaegh, F.Y., and Ploen, S.R. (2004). A survey of spacecraft formation flying guidance and control. part ii: control. In *Proceedings of the 2004 American control conference*, volume 4, 2976–2985.

Shen, D., Sun, Z., and Sun, W. (2014). Leader-follower formation control without leader's velocity information. *Science China Information Sciences*, 57(9), 1–12.

Skjetne, R., Moi, S., and Fossen, T.I. (2002). Nonlinear formation control of marine craft. In *Proceedings of the 41st IEEE Conference on Decision and Control, 2002.*, volume 2, 1699–1704.

Trinh, M.H., Oh, K.K., Jeong, K., and Ahn, H.S. (2016). Bearing-only control of leader first follower formations. *IFAC-PapersOnLine*, 49(4), 7–12.

Trinh, M.H., Zhao, S., Sun, Z., Zelazo, D., Anderson, B.D., and Ahn, H.S. (2018). Bearing-based formation control of a group of agents with leader-first follower structure. *IEEE Transactions on Automatic Control*, 64(2), 598–613.

Van Tran, Q., Trinh, M.H., Zelazo, D., Mukherjee, D., and Ahn, H. (2019). Finite-time bearing-only formation control via distributed global orientation estimation. *IEEE Transactions on Control of Network Systems*, 6(2), 702–712. doi:10.1109/TCNS.2018.2873155.

Zeng, A. and Liu, W. (2012). Enhancing network robustness against malicious attacks. *Physical Review E*, 85(6), 066130.

Zhao, S., Lin, F., Peng, K., Chen, B.M., and Lee, T.H. (2014). Distributed control of angle-constrained cyclic formations using bearing-only measurements. *Systems & Control Letters*, 63, 12–24.

Zhao, S. and Zelazo, D. (2015). Bearing rigidity and almost global bearing-only formation stabilization. *IEEE Transactions on Automatic Control*, 61(5), 1255–1268.

Zhao, S. and Zelazo, D. (2019). Bearing rigidity theory and its applications for control and estimation of network systems: Life beyond distance rigidity. *IEEE Control Systems Magazine*, 39(2), 66–83.